Structure and Oxygen Permeability of Ag-Doped $SrCo_{0.8}Fe_{0.2}O_{3-\delta}$ Oxides

Liang Tan, Li Yang, Xuehong Gu, Wanqin Jin, Lixiong Zhang, and Nanping Xu
Membrane Science and Technology Research Center, Nanjing University of Technology, Nanjing 210009, P.R. China

The powders of $SrCo_{0.8}Fe_{0.2}O_{3-\delta}$ (SCF) and SCF doped with a different amount of Ag cation are synthesized by a solid-state reaction method and the corresponding membranes are prepared. XRD results show that the doped Ag promotes the formation of a perovskite structure. The dissolution of Ag_2O into the SCF matrix results in a decreasing lattice constant with the increasing Ag content. The doping of Ag can increase the surface exchange rate and decrease the activation energy of the SCF membrane. The oxygen permeability of the Ag-doped SCF membrane is mainly influenced by both the reduction of the oxygen vacancy concentration and the improvement of the surface exchange, which depend on the content of the doped Ag and the operation temperature. The highest oxygen permeation flux is obtained when the mole ratio of Ag to SCF is 5%. © 2004 American Institute of Chemical Engineers *AIChE J,* 50: 701–707, 2004

Keywords: Ag, surface exchange, Perovskite oxides, oxygen permeability, crystal structure

Introduction

As one of the promising materials for the applications in solid oxide fuel cells (Steele, 1992; Ishihara et al., 1994), oxygen separation (Chen et al., 1997; Tsai et al., 1998) and membrane reactor (Xu and Thomson, 1997; Jin et al., 2000), perovskite oxides have been widely studied recently. Among these oxides, $SrCo_{0.8}Fe_{0.2}O_{3-\delta}$ was reported to be one of the highest oxygen permeable materials (Teraoka et al., 1985; Kruidhof et al., 1993; Qiu et al., 1995; Lee et al., 1997). However, a disparity between the oxygen permeability of these perovskite materials and the practical demand (Bredesen and Sogge, 1996) still exists. Various membranes with different materials and different compositions have been studied (Chen et al., 1997; Kovalevsky et al., 1998; Tsai et al., 1998; Xu and Thomoson, 1999; Kharton et al., 2000; Tichy and Goodenough, 2002). But unfortunately, up to now, the higher oxygen permeation flux than that of $SrCo_{0.8}Fe_{0.2}O_{3-\delta}$ has been little reported.

As known to us, the oxygen permeation through the perovskite membrane is generally divided into the following three steps: the adsorption of oxygen on the membrane surface under a higher oxygen partial pressure and the decomposition of O_2 to O^-; the transfer of O^- toward another surface under the gradient of the oxygen partial pressure across the membrane bulk; the formation of oxygen by the combination of two oxygen ions at the membrane surface under a reducing oxygen atmosphere and the desorption of oxygen. Therefore, it is commonly accepted that the rate limit of the oxygen permeation could be the surface exchange or the bulk diffusion.

In the case of the bulk diffusion, a higher oxygen permeation flux could be obtained by reducing the membrane thickness, for example, by coating a thin perovskite film on a porous support (Jin et al., 2001). But in the case of the surface exchange, the oxygen permeation flux could hardly be increased by reducing the membrane thickness. Even for the former, the influence of the surface exchange should be taken into account when the membrane thickness is reduced below a critical value (Bouwmeester et al., 1994). Surface modification has been proven to be an effective approach to improve the rate of the surface exchange between O_2 and O^-, by which a higher oxygen permeation flux was obtained (Kharton et al., 2002).

Therefore, increasing the rate of the surface exchange, which is commonly achieved by surface modification, is thought to be

Correspondence concerning this article should be addressed to N. Xu at timeforu@163.com.

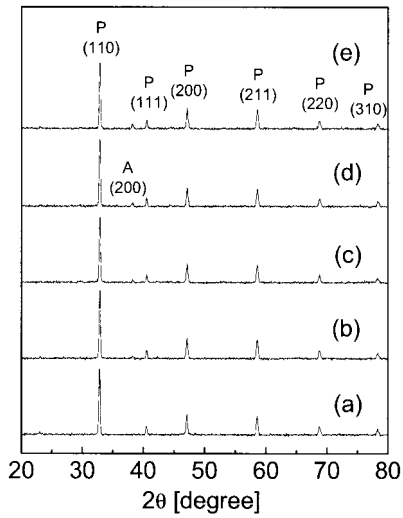

Figure 1. XRD patterns of (a) SCF, (b) SCF-Ag-2.5, (c) SCF-Ag-5, (d) SCF-Ag-7.5, and (e) SCF-Ag-10 powders calcined at 1223 K for 5 h; P (hkl): perovskite (Miller Index); A: Ag_2O.

an important means to enhance the oxygen permeability. However, considering the complicated process (Ziehfreund and Mailer, 1996; Schwartz, 1997; Hong et al., 2000) and the probable defect resulting from the shrinkage mismatch between the membrane matrix and the surface modification layer, the difficulty in using surface modification in industrial application is clear. A simple and easy-to-be-controlled method thus needs to be considered as an alternative route for the surface modification. As one of the commonly used techniques, doping could be the feasible way, if the doping material could increase the surface exchange rate of the membrane.

As reported by Bouwmeester et al. (1994) and Qiu et al. (1995), the oxygen permeation across a $SrCo_{0.8}Fe_{0.2}O_{3-\delta}$ (SCF) membrane was limited by the surface exchange. Also, because of its high oxygen permeability, SCF was thus chosen to be the membrane matrix. Kharton et al. (2002) observed that the oxygen permeation flux of the $La_{0.3}Sr_{0.7}CoO_{3-\delta}$ membrane, whose surface is modified with metal Ag, was higher than that of an unmodified $La_{0.3}Sr_{0.7}CoO_{3-\delta}$ membrane. Therefore, Ag cation is chosen as the doping ion. The objective of this study is to investigate whether the doping of Ag can increase the surface exchange rate and consequently improve the oxygen permeability of the SCF membrane. The crystal structure and the phase stability of the Ag-doped SCF oxides were also studied.

Experimental Studies

The powders were synthesized by the conventional solid-state reaction method. Stoichiometric $SrCo_3$, Co_2O_3, Fe_2O_3, and various amounts of Ag_2CO_3 were mixed and ball-milled in deionized water for 24 h. The resulting slurry was dried at 373 K for 24 h and calcined at 1223 K for 5 h to get the powders. The mole rates of Ag cation to SCF were controlled to be 2.5%, 5%, 7.5%, and 10%, and the corresponding powders were denoted as SCF-Ag-2.5, SCF-Ag-5, SCF-Ag-7.5, and SCF-Ag-10, respectively. Undoped SCF powders were also synthesized under the same conditions as those in the synthesis of Ag-doped SCF powders. The powders obtained were uniaxially pressed under 400 MPa to prepare the green disks. Membranes were prepared by sintering these green disks at 1473 K for 5 h. Preparation of the samples (powders and membranes) was performed in static air, and the heating rate was controlled to be 2 K/min. The membranes were cooled from the sintering temperature to 1223 K at a rate of 2 K/min, and then the stove was shut down. Except for the calcination of the powders, the stove was directly shut down at the end of the dwell time so that the samples were cooled naturally to the ambient temperature.

Simultaneous thermogravimetry and differential scanning calorimetry (TG–DSC; NETZSCH STA409) were performed in He flowing at 30 mL/min with a heating rate of 10 K/min. X-Ray diffraction (XRD; Bruker D8 Advance) was used to characterize the crystal structures of the powders. To investigate the phase stabilities of the materials in reducing the oxygen atmosphere, an annealing experiment was carried out as follows. The calcined powders were placed into a quartz tube and then heated to 1123 K at a rate of 2 K/min. After 5 h, the quartz tube was taken out of the stove and quenched to about 350 K by a fanner. Then, the samples were immediately differentiated by XRD. In the quartz tube, a flow of He of 30 mL/min was maintained for the entire annealing process. Oxygen permeation measurement was conducted on the high temperature oxygen permeation apparatus in our laboratory (Li et al., 1999). Before the oxygen permeation experiments, all the membranes were polished to a uniform thickness of 1.5 mm. The measurement was repeated three times, and the maximum relative error of the oxygen permeation fluxes was about 7%.

Results and Discussion

Development of the crystal structure

Figure 1 shows the XRD patterns of the powders calcined at 1223 K. The phase with the distinct diffraction peak at about 38° of the Ag-doped SCF is seen to be Ag_2O. The intensity of the diffraction peak reflects the content of the corresponding phase. Therefore, it could be deduced that the increasing amount of the doped Ag results in an increase in the content of the Ag_2O phase. It also could be seen that the doping of Ag has very little effect on the perovskite structure of SCF due to the

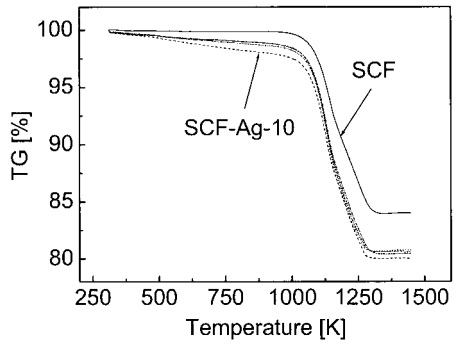

Figure 2. TG curves of SCF, SCF-Ag-2.5, SCF-Ag-5, SCF-Ag-7.5, and SCF-Ag-10 powders dried at 373 K; SCF-Ag-2.5, SCF-Ag-5, and SCF-Ag-7.5 are not indicated in the figure.

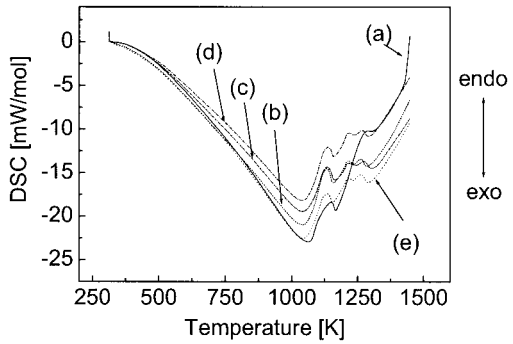

Figure 3. DSC curves of (a) SCF, (b) SCF-Ag-2.5, (c) SCF-Ag-5, (d) SCF-Ag-7.5, and (e) SCF-Ag-10 powders dried at 373 K.

similar characteristic diffraction peaks of the perovskite phase of all the oxides as shown in Figure 1.

Figure 2 shows the TG curves of the powders dried at 373 K. Because they are very close to each other, the TG curves of SCF-Ag-2.5, SCF-Ag-5, and SCF-Ag-7.5 are not shown. A sharp decline in the weight loss begins at about 1000 K and ends at about 1300 K. Figure 3 shows the DSC curves of the powders dried at 373 K. The starting temperature of the first peak and the ending temperature of the last peak are about 1050 K and 1300 K, respectively, which are similar to those shown in Figure 2. Figure 4 shows the XRD patterns of the powders calcined at various temperatures. As shown in Figure 2, the TG curves of SCF-Ag-2.5, SCF-Ag-5, and SCF-Ag-7.5 are close to each other; therefore, among these three oxides, only SCF-Ag-5 is chosen for Figure 4.

By viewing Figures 2, 3, and 4, we can observe the different development of the crystal structures of the oxides. For SCF, there are no distinct weight loss and endothermic or exothermic peak before about 1000 K, as shown in Figure 2 and Figure 3, respectively. It thus can be deduced that no distinct crystal structure transformation occurs in this temperature range, which is verified by the similar XRD patterns of the SCF powders dried at 373 K and calcined at 973 K, as shown in Figure 4a. Division of the diffraction peaks at about 26 degrees and the increase in the intensities of the diffraction peaks at about 33 degrees could be seen for SCF-Ag-5 (Figure 4b) and SCF-10 (Figure 4c). The former corresponds to the increase in the crystallinity of $SrCO_3$, and the later is attributed to the primary formation of the perovskite structure. This transformation is reflected in Figure 2, in which all the Ag-doped SCF oxides show some weight loss before about 1000 K. After calcination at 1123 K, SCF-Ag-10 shows a perfect perovskite structure, while there is still a miscellaneous peak with a distinct diffraction peak at about 30 degrees in the XRD pattern of SCF-Ag-5. As for the undoped SCF, only the powders calcined at 1223 K show the perovskite structure. Therefore, it can be concluded that the doping of Ag is instrumental in the formation of the perovskite structure. Figure 3 also shows that the DSC curves of all the Ag-doped SCF powders have their first endothermic peaks at lower temperatures than the undoped SCF oxides, which verifies the conclusion made earlier.

It can be seen from Figure 4b and 4c that the Ag_2O phase disappears in the XRD patterns of the SCF-Ag-5 and SCF-Ag-10 powders calcined at 1273 K. Ag^+ can partially substitute for the A cation of the perovskite, as reported by some authors (Choudhary et al., 1999; Song et al., 1999; Tang et al., 2000; Kania and Miga, 2001), and this substitution should not be excluded when SCF is doped with Ag. After the partial substitution of Sr^{2+} by Ag^+, the SrO phase would precipitate. Figure 4b and 4c show no such a phase existing. One probable interpretation is that the amount of partial substitution is very slight, so that the content of SrO phase is beyond the range of XRD. Another is that the partial substitution does not happen at all. In the present work, the first case is thought to be more likely, although no SrO phase could be detected. Therefore, the disappearance of the Ag_2O phase could not be entirely caused by the partial substitution of Sr^{2+} by Ag^+. Solid solution is known to be a general form for a material that consists of different oxides. The dissolution of the Ag_2O into the SCF matrix is thus thought to be the main reason for the disappearance of the Ag_2O phase. The second endothermic peak of the DSC curves of the Ag-doped SCF powders shown in Figure 3 is thought to correspond to this dissolution.

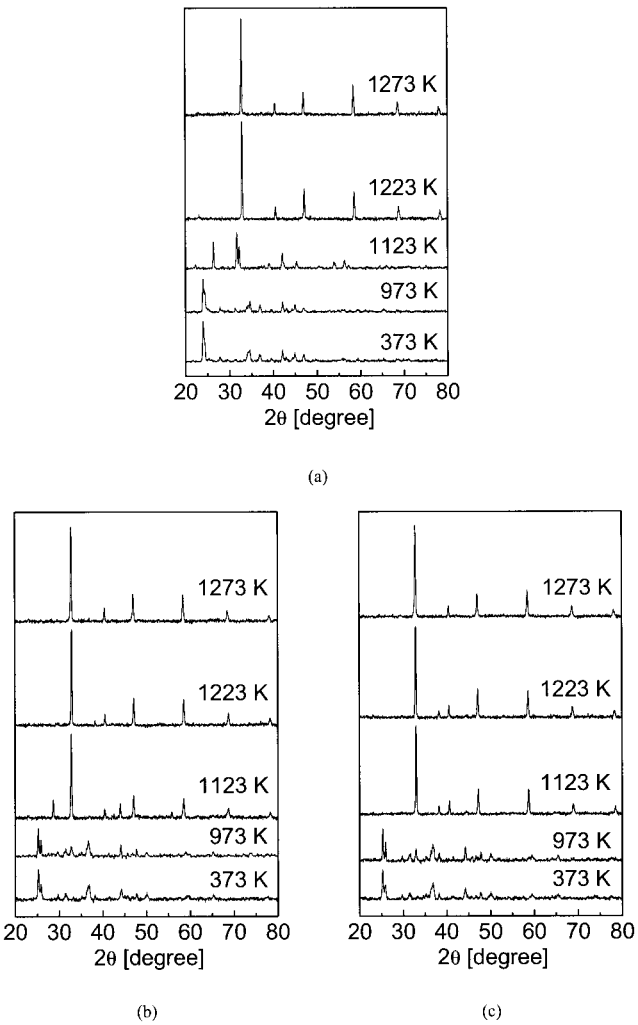

Figure 4. XRD patterns of (a) SCF, (b) SCF-Ag-5, and (c) SCF-Ag-10 calcined at various temperatures for 5 h.

Table 1. Lattice Constants of the Different Oxides Calcined at 1273 K

Oxides	Lattice Constants (10^{-10} m)
SCF	3.8642
SCF-Ag-2.5	3.8632
SCF-Ag-5	3.8625
SCF-Ag-7.5	3.8620
SCF-Ag-10	3.8611

Analysis of the lattice constant

Note that the Ag-dope SCF powders show mixed phases of perovskite and Ag_2O after being calcined at 1223 K, while they only show the perovskite structures after being calcined at 1273 K. The powders calcined at 1273 K are thus chosen to investigate the microscopic change when SCF is doped with Ag, and the lattice constants of the oxides are listed in Table 1. The lattice constants are calculated from the *d*-values of the characteristic diffraction peaks along the (110), (111), (200), (211), (220), and (310) surfaces, which are obtained directly from XRD differentiation.

It can be seen that the lattice constant of the Ag-doped SCF is smaller than that of the undoped SCF. A transformation of Co^{3+} to Co^{4+} should occur to maintain the electric neutrality when Ag^+ partially replaces Sr^{2+}. The radii of Sr^{2+} and Ag^+ of 12 coordination numbers are 1.44 and 1.40×10^{-10} m, respectively. Therefore, the partial substitution of Sr^{2+} by Ag^+, even though its degree is slight, as discussed earlier, would contribute to the reduction of the lattice constant due to the smaller ionic radii of Ag^+ and Co^{4+}.

It also can be seen from Table 1 that the lattice constant of Ag-doped SCF decreases with the increase in the content of the doped Ag. To hold electric neutrality, the dissolution of Ag_2O into the SCF matrix, as discussed earlier, would result in a reduction in the oxygen vacancy concentration. The oxygen vacancy can cause the expansion of the unit cell. Regardless of the small part of Ag^+ that partially substitutes at the A site, the doped Ag is thought to totally dissolve into the SCF matrix. The concentration of the oxygen vacancy decreases more when more Ag is doped. Therefore, the decreasing lattice constant with the increasing content of doped Ag could be interpreted. Furthermore, the smaller lattice constants of Ag-doped SCF than those of undoped SCF is also partially caused by the reduction in the oxygen vacancy concentration.

Phase stability

Figure 5 shows the XRD patterns of the calcined powders annealed in He. The splits in the diffraction peaks can be seen at about 32 and 58 degrees in the XRD patterns of all the oxides, and the degrees of these splits are similar. The phase is considered to be stable if the characteristic diffraction peaks of the perovskite phase are well maintained and the degree of the split is thought to correspond to the phase stability. Therefore, it can be deduced that the doping of Ag^+ does not obviously influence the phase stability of SCF. A gradual transformation from Co^{3+} to Co^{2+} was reported when the perovskite oxides were treated at a high temperature in a reducing atmosphere (Nakamura et al., 1979). The transformation from Co^{3+} to Co^{4+} caused by the partial substitution of Sr^{2+} by Ag^+, as discussed earlier, would result in the distortion or tilt of the

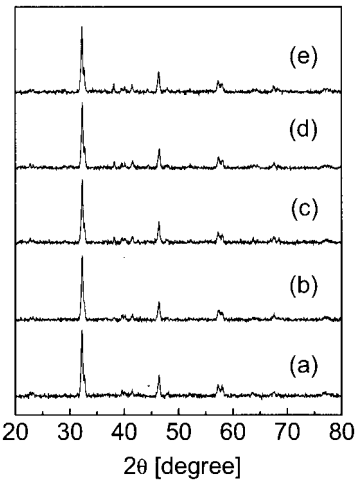

Figure 5. XRD patterns of (a) SCF, (b) SCF-Ag-2.5, (c) SCF-Ag-5, (d) SCF-Ag-7.5, and (e) SCF-Ag-10 powders annealed at 1123 K for 5 h in He.

BO_6 octahedron. It is commonly accepted that the structural stability of perovskite oxides mainly depends on the stability of the BO_6 octahedron, which consists of the B cation and the O^{2-}. However, due to its slight degree, the substitution of the Sr^{2+} by Ag^+ makes a minor contribution to the phase stability of SCF. The slight influence of the content of the doped Ag on the phase stability of SCF could also be concluded for the same reason.

Phase-transition temperature

Figure 6 shows the DSC curves of the calcined powders. It can be seen that there is an endothermic peak at about 1040 K in the DSC curve of SCF. The endothermic peak is attributed to the transition from a vacancy-ordered orthorhombic brownmillerite to a defective cubic perovskite, which was reported for the first time by Kruidhof et al. (1993). In our experiments, the phase-transition temperature is close to 1043 K, as reported by Qiu et al. (1995), but is different from the 1063 K reported by Kruidhof et al. (1993). The difference may be due to the different characterization conditions, such as the heating rate and the inert gas flow. For Ag-doped SCF, the endothermic peak appears at a temperature similar to that of SCF. This

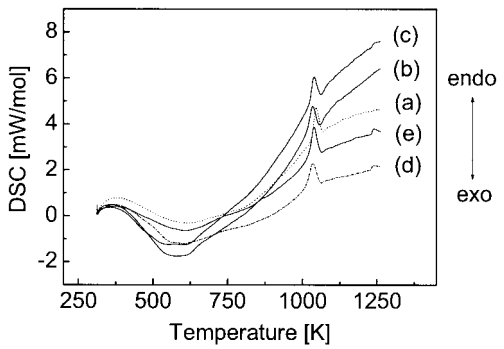

Figure 6. DSC curves of (a) SCF, (b) SCF-Ag-2.5, (c) SCF-Ag-5, (d) SCF-Ag-7.5, and (e) SCF-Ag-10 powders calcined at 1223 K.

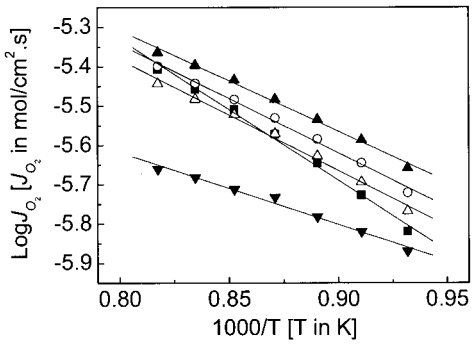

Figure 7. Arrhenius plots of oxygen permeation fluxes through (■) SCF, (○) SCF-Ag-2.5, (▲) SCF-Ag-5, (△) SCF-Ag-7.5, and (▼) SCF-Ag-10 membranes.

indicates that the doping of Ag does not obviously influence the temperature at which the phase transition occurs.

Oxygen permeability

Figure 7 shows the Arrhenius plots of the oxygen permeation fluxes of the membranes. The oxygen partial pressures at the air side and the permeation side of the membranes are kept at 0.21×10^5 Pa and 1.013×10^2 Pa, respectively. Our previous work indicated that the oxygen permeation fluxes were different for the membranes with different crystal structures (Tan et al., 2003). As shown in Figure 4, all of the powders have a similar crystal structures after being calcined at 1273 K. Consequently, the crystal structures of all the membranes are thought to be similar, because the membranes are sintered at a higher temperature, 1473 K, which is verified by the XRD characterization of the sintered membranes (not given in this article). Therefore, the influence of the crystal structures on the oxygen permeability of the membranes could be neglected. The partial substitution of Sr^{2+} by Ag^+ results in a decrease in the content of Co^{3+}. Even if it could also be neglected due to its low degree, as stated earlier, this partial substitution would reduce the oxygen loss, followed by the transformation from Co^{3+} to Co^{2+}. Ag_2O dissolves into the SCF matrix when the membranes are sintered at 1473 K. With the doping of the Ag^+ of the positive ionic valence, the concentration of the oxygen vacancy should be reduced to maintain the electric neutrality of the system. This reduction of the oxygen vacancy would result in a lower loss of the lattice oxygen.

However, the SCF-Ag-2.5 and SCF-Ag-5 membranes show higher oxygen permeation fluxes than those of the undoped SCF membrane, as shown in Figure 7. The thickness of the $SrCo_{0.8}Fe_{0.2}O_{3-\delta}$ membranes used in the works of Qiu et al. (1995) was 1.0, 2.7, and 5.5 mm, and the results showed that the permeation flux at a fixed temperature is independent of the disc thickness. Another work of Lee et al. (1997) indicated that the permeation in membranes in the thickness range of 1 to 2.6 mm was controlled both by the bulk diffusion of oxide ions and by surface exchange. In our work, the thickness of the membranes was 1.5 mm, which is in the 1- to 2.6-mm range, as reported by Lee et al. (1997). Consequently, both the bulk diffusion and surface exchange influence the overall oxygen permeation. Because the Ag-doped $SrCo_{0.8}Fe_{0.2}O_{3-\delta}$ membranes are of the same thickness, the influence of the bulk diffusion on the oxygen permeation is thought to be almost the same. Here, the increase in the surface exchange rate is thought to be the key reason that results in the higher oxygen permeation flux. For SCF-Ag-2.5 and SCF-Ag-5 membranes, the influence of the improvement in the surface exchange dominates the influence of the reduction in the oxygen vacancy concentration. Therefore, the SCF-Ag-2.5 and SCF-Ag-5 membranes show higher oxygen permeation flux than the SCF membrane. The opposite situation occurs for the SCF-Ag-10 membrane, due to the excess dissolution of Ag_2O into the SCF matrix. Therefore, the oxygen permeation of the SCF-Ag-10 membrane is lower than that of the SCF membrane, as shown in Figure 7.

Wang et al. (2000) reported that the doping of Ag_2O in the $La_{0.6}Sr_{0.4}MnO_3$ could result in plenty of oxygen species that could be desorbed at the relatively low temperature. The work of Choudhary et al. (1999) also showed that the partial substitution of La by Ag could increase the catalytic activity of undoped $LaFeO_3$ and $LaFe_{0.5}Co_{0.5}O_3$ at a low temperature. In our experiment, although the existing form of Ag^+ is different from that in the preceding two works, the same trend is inferred. In order to clearly understand the effect of temperature on the improvement of the surface exchange caused by the doping of Ag, we plot the curves of the relative difference (using symbol *RJ* as a representative) in the oxygen permeation flux between the Ag-doped and the undoped SCF membranes as a function of temperature, which is shown in Figure 8. Here *RJ* is calculated to be $RJ = (J - J_0)/J_0 \times 100\%$, where J and J_0 are the oxygen permeation flux of the Ag-doped and undoped SCF membranes, respectively.

It can be seen in Figure 8 that for all the Ag-doped SCF membranes, *RJ* decreases with the increase in the temperature. For SCF-Ag-5, when the temperature is increased from 1073 K to 1223 K, *RJ* decreases from 44.6% to 10.4%. This means that the influence of the improvement in the surface exchange caused by the doping of Ag^+ on the oxygen permeability of SCF is more apparent at lower temperatures.

Compared with the undoped SCF membrane, the SCF-Ag-7.5 membrane has lower oxygen permeation fluxes at higher temperatures, but higher fluxes at lower temperatures, as shown in Figure 7. The reduction in the oxygen vacancy concentration plays a major role in determining the oxygen permeability when the SCF-Ag-7.5 membrane is at a higher temperature.

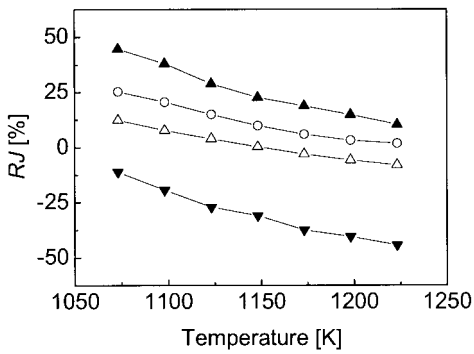

Figure 8. RJ of (○) SCF-Ag-2.5, (▲) SCF-Ag-5, (△) SCF-Ag-7.5, and (▼) SCF-Ag-10. membranes as a function of temperature.

With the decrease in the temperature, the influence of the increase in the surface exchange rate is strengthened. Thus, the comparison between the oxygen permeation fluxes of the SCF and SCF-Ag-7.5 membranes is explained.

It also can be seen from Figure 7 that for each measured temperature, with an increase in the doped Ag^+, the oxygen permeation first increases and reaches the maximum value when the content of Ag^+ is 5%, and then decreases. A related interaction between the reduction of the oxygen vacancy and the improvement of the surface exchange is thought to exist. For the SCF-Ag-5 membrane, both the reduction in the oxygen vacancy concentration and the improvement in the surface exchange are more than those of the SCF-Ag-2.5 membrane. The combined result shows the positive influence. When excess Ag^+, such as the SCF-Ag-7.5 or SCF-Ag-10 membrane, is doped, the combinative result is negative. In our experiment, the optimal content of doped Ag^+ is 5%.

The calculated activation energies are 68.9, 53.0, 49.2, 54.2, and 35.1 kJ/mol for SCF, SCF-Ag-2.5, SCF-Ag-5, SCF-Ag-7.5, and SCF-Ag-10 membranes, respectively. The doping of Ag significantly decreases the activation energies for oxygen permeation, which is thought to be due to the improvement of the surface exchange. The activation energy reflects the change in the oxygen permeation flux with the temperature. As stated earlier, the improvement in surface exchange caused by the doping of Ag is more apparent at lower temperatures. This would increase the slope (the slope is a negative value) of the lines shown in Figure 7. Consequently, the activation energies of the Ag-doped SCF membranes calculated from the slopes are reduced.

Conclusions

The perovskite structures of the calcined Ag-doped SCF powders are well preserved by the minor Ag_2O phase. The development of the crystal structure of Ag-doped SCF is found to be different from that of undoped SCF. The doping of Ag encourages the formation of the perovskite structure. The Ag_2O phase dissolves into the SCF matrix when the oxides are calcined at a higher temperature. Due to the reduction in the oxygen vacancy concentration caused by this dissolution, the lattice constant of the oxides decreases with the increase in the doped Ag content.

The doped Ag has a slight influence on the phase stability of SCF. The effect of doped Ag on the phase transition between brownmillerite and perovskite is also negligible.

The doping of Ag can increase the surface exchange rate of the SCF membrane. For SCF-Ag-2.5 and SCF-Ag-5 membranes, the higher oxygen permeation fluxes are attributed to the dominating influence of the improvement of the surface exchange. When SCF is doped with excess Ag, such as SCF-Ag-10, the reduction in the oxygen vacancy concentration is determinative, which results in a decrease in the oxygen permeation flux. The highest oxygen permeation flux is obtained when the mole rate of the doped Ag to SCF is 5%. It is found that at lower temperatures, the improvement in the surface exchange is more remarkable. The doping of Ag also can decrease the activation energy for oxygen permeation.

Acknowledgments

We acknowledge the support of the National Natural Science Foundation of China (NNSFC, No. 20125618) and the Key Laboratory of Materials-Oriented Chemical Engineering and Technology of Jiangsu Province.

Literature Cited

Bouwmeester, H. J. M., H. Kruidhof, and A. J. Burggraaf, "Importance of the Surface Exchange Kinetics as Rate Limiting Step in Oxygen Permeation Through Mixed-Conducting Oxides," *Solid State Ionics,* **72,** 185 (1994).

Bredesen, R., and J. Sogge, paper presented at The United Nations Economic Commission for Europe Seminar on Ecological Applications of Innovative Membrane Technology in Chemical Industry, Cetaro, Calabria, Italy (1996).

Chen, C. H., H. J. M. Bouwmesster, R. H. E. van Doorn, H. Kruidhof, and A. J. Burggraaf, "Oxygen Permeation of $La_{0.3}Sr_{0.7}CoO_{3-\delta}$," *Solid State Ionics,* **98,** 7 (1997).

Choudhary, V. R., B. S. Uphade, and S. G. Pataskar, "Low Temperature Complete Combustion of Methane over Ag-Doped $LaFeO_3$ and $LaFe_{0.5}Co_{0.5}O_3$ Perovskite Oxide Catalysts," *Fuel,* **78,** 919 (1999).

Hong, L., X. Chen, and Z. Cao, "Preparation of a Perovskite $La_{0.2}Sr_{0.8}CoO_{3-x}$ Membrane on a Porous MgO Substrate," *J. Eur. Ceram. Soc.,* **21,** 2207 (2000).

Ishihara, T., H. Matsuda, and Y. Takita, "Doped-$LaGaO_3$ Perovskite Type Oxide as a New Oxide Ionic Conductor," *J. Amer. Chem. Soc.,* **116,** 3801 (1994).

Jin, W., S. Li, P. Huang, N. Xu, and J. Shi, "Preparation of an Asymmetric Perovskite-Type Membrane and Its Oxygen Permeability," *J. Membr. Sci.,* **185,** 237 (2001).

Jin, W., X. Gu, S. Li, P. Huang, N. Xu, and J. Shi, "Experimental and Simulation Study on a Catalyst Packed Tubular Dense Membrane Reactor for Partial Oxidation of Methane to Syngas," *Chem. Eng. Sci.,* **55,** 2617 (2000).

Kania, A., and S. Miga, "Preparation and Dielectric Properties of $Ag_{1-x}Li_xNbO_3$ (ALN) Solid Solutions Ceramics," *Mater. Sci. Eng. B,* **86,** 128 (2001).

Kharton, V. V., A. P. Viskup, A. V. Kovalevsky, F. M. Figueiredo, J. R. Jurado, A. A. Yaremchenko, E. N. Naumovich, and J. R. Frade, "Surface-Limited Ionic Transport in Perovskite $Sr_{0.97}(Ti,Fe,Mg)O_{3-\delta}$," *J. Mater. Chem.,* **10,** 1161 (2000).

Kharton, V. V., A. V. Kovalevsky, A. A. Yaremchenko, F. M. Figueiredo, E. N. Naumovich, A. L. Shaulo, and F. M. B. Marques, "Surface Modification of $La_{0.3}Sr_{0.7}CoO_{3-\delta}$ Ceramic Membranes," *J. Membr. Sci.,* **195,** 277 (2002).

Kovalevsky, A. V., V. V. Kharton, V. N. Tikhonovich, E. N. Naumovich, A. A. Tonoyan, O. P. Reut, and L. S. Boginsky, "Oxygen Permeation Through $Sr(Ln)CoO_{3-\delta}$ (Ln = La, Nd, Sm, Gd) Ceramic Membranes," *Mater. Sci. Eng. B,* **52,** 105 (1998).

Kruidhof, H., H. J. M. Bouwmeester, R. H. E. van Doorn, and A. J. Burggraaf, "Influence of Order-Disorder Transitions on Oxygen Permeability Through Selected Nonstoichiometric Perovskite-Type Oxides," *Solid State Ionics,* **63/65,** 816 (1993).

Lee, T. H., Y. L. Yang, A. J. Jacobson, B. Abeles, and M. Zhou, "Oxygen Permeation in Dense $SrCo_{0.8}Fe_{0.2}O_{3-\delta}$ Membranes: Surface Exchange Kinetics Versus Bulk Diffusion," *Solid State Ionics,* **100,** 77 (1997).

Li, S., W. Jin, P. Huang, N. Xu, J. Shi, M. Z.-C. Hu, E. A. Payzant, and Y. H. Ma, "Perovskite-Related ZrO_2-Doped $SrCo_{0.4}Fe_{0.6}O_{3-\delta}$ Membranes for Oxygen Permeation," *AIChE J.,* **45,** 276 (1999).

Nakamura, T., G. Petzow, and L. J. Gauckler, "Stability of the Perovsktie Phase $LaBO_3$ (B = V, Cr, Mn, Fe, Co, Ni) in Reducing Atmosphere. 1. Experimental Results," *Mater. Res. Bull,* **14,** 649 (1979).

Qiu, L., T. H. Lee, L.-M. Liu, Y. L. Yang, and A. J. Jacobson, "Oxygen Permeation Studies of $SrCo_{0.8}Fe_{0.2}O_{3-\delta}$," *Solid State Ionics,* **76,** 321 (1995).

Schwartz, R. W., "Chemical Solution Deposition of Perovskite Thin Films," *Chem. Mater.,* **9,** 2325 (1997).

Song, K. S., H. X. Cui, S. D. Kim, and S. K. Kang, "Catalytic Combustion of CH_4 and CO on $La_{1-x}M_xMnO_3$ Perovskites," *Catal. Today,* **47,** 155 (1999).

Steele, B. C. H., "Oxygen Ion Conductors and Their Technological Applications," *Mater. Sci. Eng.,* **B13,** 79 (1992).

Tan, L., X. Gu, L. Yang, L. Zhang, C. Wang, and N. Xu, "Influence of

Sintering Condition on Crystal Structure, Microstructure, and Oxygen Permeability of Perovskite-Related Type $Ba_{0.8}Sr_{0.2}Co_{0.8}Fe_{0.2}O_{3-\delta}$ Membranes," *Sep. Purif. Technol.,* **32,** 307 (2003).

Tang, T., K. M. Gu, Q. Q. Cao, D. H. Wang, S. Y. Zhang, and Y. W. Du, "Magnetocaloric Properties of Ag-Substituted Perovskite-Type Manganites," *J. Magn. Magn. Mater.,* **222,** 110 (2000).

Teraoka, Y., H.-M. Zhang, and N. Yamazoe, "Oxygen Permeation Through Perovskite-Type Oxides," *Chem. Lett.,* 1743 (1985).

Tichy, R. S., and J. B. Goodenough, "Oxygen Permeation in Cubic $SrMnO_{3-\delta}$," *Solid State Sci.,* **4,** 661 (2002).

Tsai, C. Y., A. G. Dixon, Y. H. Ma, W. R. Moser, and M. R. Pascucci, "Dense Perovskite, $La_{1-x}A_xFe_{1-y}Co_yO_{3-\delta}$(A′ = Ba, Sr, Ca), Membrane Synthesis, Applications, and Characterization," *J. Amer. Ceram. Soc.,* **81,** 1437 (1998).

Wang, W., H.-B. Zhang, G.-D. Lin, and Z.-T. Xiong, "Study of Ag/$La_{0.6}Sr_{0.4}MnO_3$ Catalysts for Complete Oxidation of Methanol and Ethanol at Low Concentrations," *Appl. Catal. B: Environ.,* **24,** 230 (2000).

Xu, S. J., and W. J. Thomson, "Oxygen Permeation Rates Through Ion-Conducting Perovskite Membranes," *Chem. Eng. Sci.,* **54,** 3839 (1999).

Xu, S. J., and W. J. Thomson, "Perovskite-Type Oxides Membranes for the Oxidative Coupling of Methane," *AIChE J.,* **43,** 2731 (1997).

Ziehfreund, A., and W. F. Maier, "Preparation of Ultrathin Supported Solid Electrolyte Membranes for Oxygen Separation," *Chem. Mater.,* **8,** 2721 (1996).

Manuscript received Feb. 15, 2003, and revision received June 18, 2003.